Functional Imaging of Compressed Breast by Microwave Radiometry

S. Iudicello and F. Bardati

Dipartimento di Informatica Sistemi e Produzione,
Università di Roma Tor Vergata, via del Politecnico 1,Roma, Italy, 00133

Abstract **–** A tumor is visible by a passive microwave radiometer scanning the breast surface if it changes the radiometer output of a healthy breast to an extent that overcomes the radiometric resolution for the given sensing antenna and integration time. In this paper the breast is intentionally squeezed between the radiometric antenna and the chest wall and the temperature is evaluated for the deformed breast together with the generated radiometric signal. To be compared with the radiometric resolution, the difference signal between the outputs in the presence of a lesion and in its absence has to be evaluated. To achieve this, a mechanical, thermal and electromagnetic model of the breast has been developed. A finite-element code has been used to solve for the mechanical and thermal problems, while FDTD has been exploited for electromagnetic computations. We show that compressing the breast improves the radiometric visibility depending on tumor depth and deformation.

I. INTRODUCTION

In principle microwave radiometry, i.e. passive detection of spontaneous thermal radiation from a body in the microwave frequency band can provide information on the thermal status of tissues to a depth of some centimeters [1]. In clinics, microwave radiometry has been considered in the attempt to cope with two major challenges, i. e. non-invasive temperature monitoring during thermal treatment of extended regions of tissue, and early detection of tumor malignancies. First-type applications have been proposed in [2,3] and, recently, revived in connection with a curtain of radiofrequency radiators for antitumoral hyperthermia treatment of chest wall recurrences [4]. The diagnostic application has been investigated also in connection with the problem of retrieving a temperature profile from a set of radiometric data [5-8]. In spite of some positive evidence, however, microwave radiometry has not yet reached a general consensus as a screening modality for early detection of cancer although recent results seem encouraging [9]. A renewed interest in clinical microwave radiometry can be explained on the basis of the improved performance of both microwave instrumentation and computer modeling of complex systems.

During a typical session a contacting antenna scans the surface of a breast. When a thermal anomaly is located within the radiation solid of the antenna, i. e. the volume of breast that contributes almost all the net real power entering the antenna from the breast, the receiver output increases to some amount. The anomaly is radiometrically visible if such amount is larger than the instrumental resolution. In spite of the simplicity of the underlying rationale, measurements on patients may fail because inadequacies of the instruments and presence of artifacts due to spurious radiation. When the antenna explores the breast, in fact, the data may vary because any change in the antenna match causes a variation in the back reflection of thermal noise from the receiver. An ideal radiation-balance radiometer [10] prevents this drawback. Moreover, the increment in received power due to a visible thermal anomaly must overcome the floor power due to thermal emission from normal tissue. A parametric study on the radiometric visibility of thermal anomalies has been presented in [11] for an elementary antenna consisting of a circular aperture in a perfectly conducting screen. An improved model of breast, which includes a portion of chest and a skin layer, has been considered in [12]. The results of these investigations show that a 10mm spherical lesion is radiometrically visible by a system with 0.1 C° resolution if it is not deeper than 2.5cm. When a contacting sensor is scanned on the breast a pressure is normally exercised. The breast is deformed so that the distance of a lesion from the contacted surface is lowered while its visibility is changed. While breast flattening has been treated as a negligible effect in the modeling by previous authors, in this paper the breast is intentionally squeezed between antenna and thorax and we estimate the thermal behavior and the corresponding radiometric signal for the deformed breast. Breast compression is routinely performed during compression mammography to an extent that is indicated by regulatory agencies [13].

For the signal S in output to a radiation balance microwave radiometer we shall use,

$$S = \int_{\Omega} W(\underline{r}) T(\underline{r}) dV \qquad (1)$$

where W is called weighting function, T is the physical temperature and Ω is the overall volume that is sensed by the antenna. Due to reciprocity in antenna theory W can be obtained as,

$$W(\underline{r}) = \frac{P_d(\underline{r})}{\int_{\Omega} P_d(\underline{r})dV} \tag{2}$$

where $P_d(\underline{r})$ is microwave power deposition at point $\underline{r} \in \Omega$ when the antenna radiates onto the body in active modality [14]. The presence of a malignancy may result in an excess of temperature ΔT as well as in a change ΔP_d within Ω, due to a change in permittivity of tumor tissue with respect to normal tissue. The radiometric resolution (sensitivity) will be denoted by δS. In the next Section the breast deformation due to a compression exercised normally to the chest wall will be studied, while the thermal and electromagnetic models that are necessary to estimate S will be presented in Section III. The mechanical and thermal problems have been solved in a finite-element frame using the commercial tool COMSOL Multiphysics [15]. The electromagnetic problems have been solved by FDTD using a proprietary code. Preliminary results will be presented showing the increase in visibility that are consequent to breast compression.

II. BIOMECHANICAL MODEL

To evaluate the radiometric signal the mechanical, thermal and electromagnetic properties of the breast must be specified for each tissue component. The normal breast consists of a tree-like structure of glandular tissue supported by connective tissue, immersed in fat and surrounded by skin. However, to simplify the problem, we model the breast as a homogeneous hemisphere supported by a square box of muscle (Fig. 1). Assuming that the breast is made of an equal amount of fat and glandular tissue, the homogeneous model results from averaged mechanical properties.

To model the breast deformation under compression, a simulation model, which can handle large deformations and nonlinear, nearly incompressible materials, must be implemented. In literature breast-deformation modeling is receiving attention due to the need of data fusion from X-ray mammography in different views and Magnetic Resonance Imaging in early cancer diagnostics as well as to achieve suitable information for surgery or needle insertion during a biopsy [16-20]. Biological tissues have been shown to exhibit non-linear stress-strain laws [21, 22] and this is the case for the range of strains involved during mammographic screens. Different material models for breast tissues are proposed in the literature. A review of strain-stress relationships can be found in [17]. The resulting stress for a given strain is largely dependent on the model, while a criterion for model validation can be the plausibility of the achieved deformation in the comparison with experimental outcomes. E.g. in [23] the displacement of a set of landmarks positioned on a patient has been measured for increasing net deformation. The exponential models are more accurate than linear and neo-hookean ones in retrieving large breast deformation. However, as a drawback, they originate non-realistic compression forces [23,24].

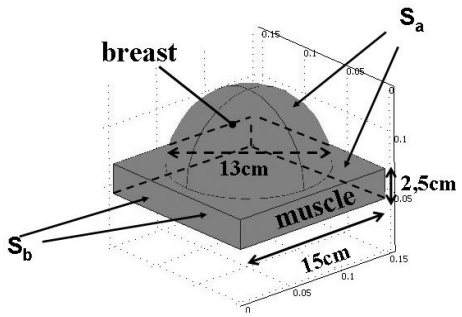

Fig. 1. Hemispherical model of undeformed breast on a muscle box.

The kinematic problem is to find the coordinates $\underline{x}$ of the deformed body, given the coordinates $\underline{X}$ of the undeformed body. The displacement vector and the Green-Lagrange strain tensor are respectively defined as,

$$\underline{U} = \underline{x} - \underline{X} \tag{3}$$

$$E_{ij} = \frac{1}{2}\left(\frac{\partial U_i}{\partial X_j} + \frac{\partial U_j}{\partial X_i} + \frac{\partial U_k}{\partial X_i}\frac{\partial U_k}{\partial X_j}\right) \tag{4}$$

where summation over repeated indices is intended. The deformation gradient tensor $F_{ij} = \partial x_i / \partial X_j$ is introduced. The Second Piola-Kirchoff tensor, T_{mn}, is generally used as stress definition in large deformation problems. T_{mn} is defined as the force acting on the undeformed body measured per unit undeformed area. In an equilibrium deformed state, all forces must balance, and it can be shown that this leads to,

$$\frac{\partial}{\partial X_m}\left(T_{mn}\frac{\partial x_i}{\partial X_n}\right) + f_i = 0, \quad (i = 1, 2, 3) \tag{5}$$

where f_i is volume external force component per unit volume. To relate stress to strain, a strain energy function $W(E_{ij})$ is assumed to exist. The principle of virtual works allows the equilibrium problem (5) to be reformulated as an energy minimization problem. We have made the assumption that the tissue is isotropic. If a material is isotropic, the strain-energy density function W can be in general expressed as a function of the strain invariants I_1, I_2, I_3 where $I_1 = tr(F_{ij}^T F_{ij})$ and ^{T} is for transposed. $I_3 = J^2$, with J volume ratio. $J = 1$ for a perfectly incompressible material. Practically, tissues have a Poisson's ratio that ranges from 0.49 to 0.5. The Poisson's ratio for the tissue used in this study is 0.498. We assumed an exponential constitutive law [18],

$$W = a(e^{b(I_1-3)} - 1) - \frac{p}{2}(I_3 - 1) \qquad (6)$$

where a and b are average fit parameters between fat and glandular tissue calculated from uniaxial stress-strain experiments using a tissue sample [25], p is the internal pressure that represents a Lagrangian multiplier introduced to impose the constraint $I_3 - 1 = 0$.

Finally, the mechanical boundary conditions must be specified to obtain the solution. We admit that the radiometric antenna is frontally pressed against the breast, which is squeezed between the planar antenna and the thorax plane, coincident with the pectoral muscle wall. The two planes are parallel. The muscle wall is fixed. Zero displacement on the muscle wall in contact with the breast and zero pressure on the free skin surface are suitable boundary conditions. The antenna itself has been modeled as a compression plate with the mechanical coefficients of aluminum. At the interface between antenna and breast a non-penetration condition holds [18]. Owing to this condition the breast modeling under compression is not a standard elasticity problem. Let D be the distance of the antenna plate from the chest wall. The compression plate is supposed to move in the direction of the z-axis, towards the chest. D equals the hemisphere radius R in the undeformed configuration, when the plane is contacting the breast at a single point (Fig. 2(a)). During compression D is reduced while the plate/breast contact area increases (Fig. 2(b)). If the total displacement of the plate is C, then the relative net deformation is $C/R=(R-D)/R$. The following numerical analysis will be performed for a net deformation of 35%, which is between the limit values of mammography (20-50%). In order to model such a large deformation we divided C into N small displacements. Then we solved N linear deformation problems as a sequence of steps. At the end of each step, we know the flattened breast surface in contact with the antenna. However, we don't know 'a priori' which additional surface the antenna will contact as a consequence of the deformation at the next step. The problem of determining the additional contact surface of a deformable body under compression is known as a contact analysis problem. It has been formulated and solved as an Augmented Lagrangian optimization [26].

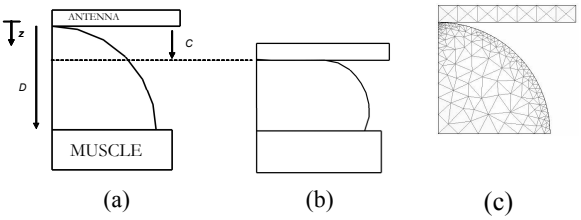

Fig. 2. a) Geometry of the undeformed breast, sagittal view. b) Geometry of the deformed breast. c) Undeformed breast. Partition into triangular elements.

Due to axial symmetry a quarter of the structure has been modeled, therefore the further condition of zero displacement normally to the symmetry walls has been introduced. The finite-element mesh consists of 15150 tetrahedral elements, 14620 for the breast and 530 for the compression plate. A view of the partition into elements is shown in Fig. 2(c). Mesh density is higher near the initial point of contact between the breast and the antenna while an element size of 2.5 mm is specified on the breast external surface. To solve for the non-linear mechanical behavior, after a small displacement increment of the compression plate, the internal pressure is computed together with the displacement at each point.

In mammography breast deformation studies, the relative reduction of a breast diameter is imposed, while the net force between the plates is computed from the resulting stress. The diagram in Fig. 2(b) refers to a breast deformation of about 35% for frontal compression. The compression force results in about 1750 N. As expected, this value is larger than the net force experienced in X-ray mammography, which ranges between 49 and 186 N [24]. In Fig. 3 the displacement is shown versus particle depth in the undeformed state on a sagittal plane. The displacement is practically linear with depth, with 35% slope.

We modeled a tumor as a sphere. In this preliminary work the sphere is located on the symmetry axis (z-axis) perpendicular to the chest wall. Tumor-center distance from the antenna contact point in the undeformed state is referred to as tumor depth. For simplicity the mechanical properties of the tumor have been taken coincident with those of the host tissue. After frontal compression the sphere is deformed into an ellipsoid whose axes can be estimated using the diagram in Fig. 3 for the

displacements of the tumor-diameter end-points along the *z*-axis, while the two other axes are found by tumor volume conservation.

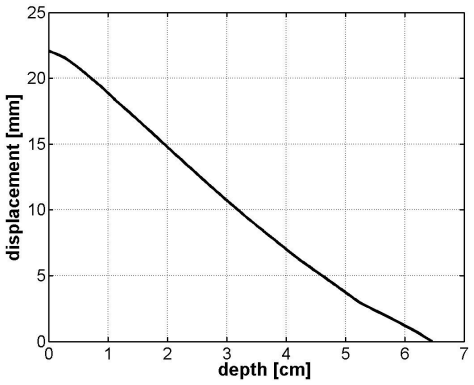

Fig. 3. Particle displacement vs. depth on *z*-axis.

III. THERMALAND ELECTROMAGNETIC MODELS

We assume the temperature satisfies the steady-state bio-heat equation,

$$\nabla \cdot \kappa \nabla T + q_m - \rho_b c_b w_b (T - T_b) = 0 \qquad (7)$$

where κ is the effective thermal conductivity which includes the enhancement in conductivity due to blood perfusion, qm is the metabolic heat generation rate, c_b is the specific heat, ρbwb is the blood perfusion rate per unit mass of tissue and T_b is the arterial blood temperature. The boundary condition at the interface S_a between breast and air is,

$$\kappa \nabla T \cdot \hat{n}_a + h_a (T - T_a) = 0 \qquad (8)$$

with $\hat{n}_a$ the unit vector normal to the boundary, h_a a heat transfer coefficient, and T_a the air temperature. T is continuous at the interface between breast and pectoral muscle. We assume an adiabatic condition $\partial T / \partial n = 0$ at the boundary S_b with the main body. The solution $T(\underline{r})$ to equations (7) and (8) is diagrammed in Fig. 4(a) on a sagittal plane for the geometry of Fig. 2.

In previous work [11,12] the contact between antenna and breast was ideally confined to a small area and to a very short time interval, in such a way to neglect temperature variations in the breast due to the soft contact with the antenna. Two limiting cases can be envisaged in the presence of large deformations. In a first case the antenna is instantaneously compressed against the breast, while the radiometer takes the data in that instant. No heat exchanges are allowed, so that the temperature of a particle at a point $\underline{\boldsymbol{x}}$ in the compressed state coincides with its temperature at the initial location $\underline{\boldsymbol{X}}$ in the undeformed state (Fig. 4(b)). We shall refer to this temperature as adiabatic temperature. In a second case, the radiometric data acquisition takes enough time (about 15 minutes as shown in Fig. 5) to let the temperature reach the steady state within the deformed breast in the presence of a larger contact surface between antenna and breast (Fig. 4(c)). We shall refer to this temperature as steady-state temperature. We expect that the temperature that is sensed by the antenna during a realistic measurement be between these limiting cases. The heat transfer coefficient is assumed h_a=13.5 W/(m^2·K) [27], at the breast/air interface. At the boundary between antenna and breast, equation (8) still holds, with a heat transfer coefficient h_a=135 W/(m^2·K), i.e., ten times the coefficient for the air/breast interface. The antenna is supposed to be kept at a reference temperature T_a, by circulating de-ionized water.

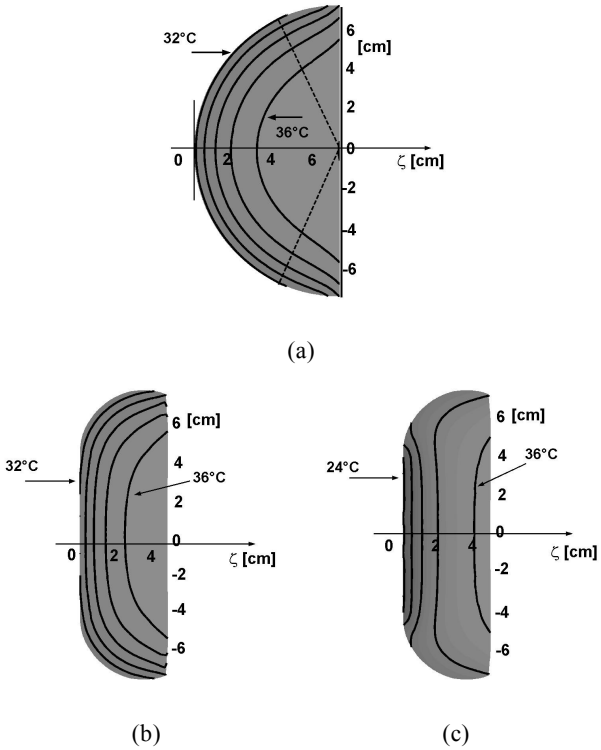

Fig. 4. a) Isotherms (step 1°C) on a sagittal plane for undeformed normal breast. b) Isotherms (step 1°C) for deformed normal breast in the adiabatic case. c) Isotherms (step 3°C) for deformed normal breast in the steady-state case. For normal breast: κ=0.48W/m·°C, q_m=700 W/m^3, ρ_b=1060 Kg/m^3, c_b=2600 J/Kg·°C, w_b=0.00054 s^{-1}. For muscle: κ=0.48 W/m·°C, q_m=700 W/m^3, w_b=0.0008 s^{-1}. T_a=20°C, T_A=20°C, T_b=37°C.

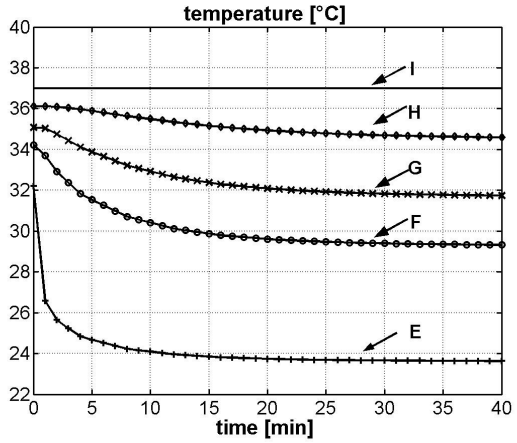

Fig. 5. Temperature T vs. time at the points labeled as in Fig. 2(b). The curves start for t=0 from the adiabatic values.

A tumor may change *T(r)* into a new temperature *T'(r)* differing by $\Delta T(r)$ from the normal breast temperature mainly in the tumor volume and in the surrounding tissue. Thermogenesis and angiogenesis are considered responsible for this change [28]. Thermogenesis is accounted for by a value qm that is related to the tumor doubling time by a hyperbolic law, while the tumor size is exponentially related to the doubling time [29]. Diagrams of ΔT vs. lesion depth are shown in Fig. 6 along a line through the lesion center, for a 10 mm tumor centered at 1cm, 2cm, 3cm and 4cm from the surface, in the adiabatic and steady-state cases. The tumor depth is the tumor-center distance from the surface before compression.

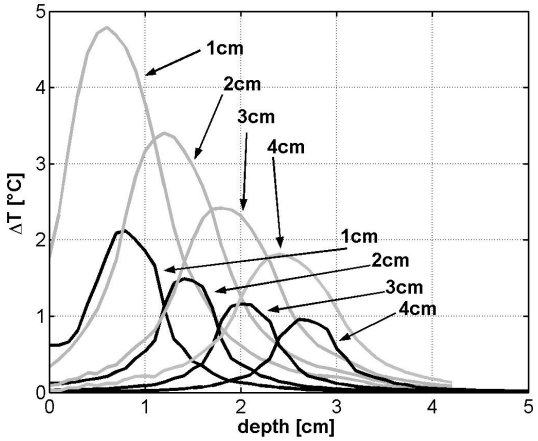

Fig. 6. Temperature difference (unhealthy-normal) ΔT for a 10mm lesion and compressed breast. Steady-state (gray line) and adiabatic (bold line) temperatures. Tumor parameters: κ_t=0.511 W/m·°C, q_{mt}=65400 W/m^3, w_{tb}=0.01 s^{-1} [27].

From the diagrams in Fig. 4 we observe that the breast peripheral temperature is lower for steady-state because of the more effective superficial cooling forced by the contacting antenna. Therefore the tumor steady-state over temperature ΔT is higher than the adiabatic one as shown in Fig. 6.

For the sake of generality we shall not specify any particular radiometric antenna letting the size be its only characteristic feature. The electromagnetic model consists of a circular aperture of diameter *2a*, center at $z = 0$, in an infinite conducting plane. We assume the half-space in front of the aperture is filled by breast tissue. Accounting for the heterogeneity of breast tissue is a difficult task since the adipose tissue is inseparably intermixed with fibroglandular parenchyma (except in the subcutaneous region) [30,31]. For simplicity we assume a homogeneous medium with dielectric properties as in [11,32]. We refer to [33] for tumor dielectric properties. Recently, the dielectric properties of normal and malignant breast tissues have been experimentally characterized in the microwave frequency range by Lazebnik *et al*. [34,35]. Basing on the percentage of adipose tissue content, they classified samples of normal breast into three groups. The dielectric properties we adopted for normal breast are similar to those in the third group in [34] (85-100% adipose tissue content).

The field is radiated by a uniform linearly-polarized electric field $\underline{E}_a$ on the aperture. The center-band frequency is 2.6 GHz, which is close to widely used frequencies in medical application of microwave radiometry [4], [36-39]. Electromagnetic field computations have been performed by a proprietary FDTD code using Mur absorbing boundary conditions at the walls. The FDTD computation has been repeated in the presence of the spherical lesion with its center at various depths. Contour-level plots of P_d are shown on two orthogonal principal planes in Fig. 7.

IV. RESULTS

The radiometric signal *S* has been computed by equation (1) after the temperature and power $\boldsymbol{P}_d$ delivered to tissue have been determined within both normal and unhealthy breast. Denote the difference between unhealthy and normal breast signals by ΔS,

$$\Delta S = \int_{\Omega} W'(\underline{r})T'(\underline{r})dV - \int_{\Omega} W(\underline{r})T(\underline{r})dV \qquad (9)$$

where the prime is used for the unhealthy breast. Therefore ΔS is a useful parameter in breast tumor detection by microwave radiometry. Diagrams of ΔS are shown in Fig. 8 as a function of tumor depth and refer to

non-compressed breast. The two curves have been obtained from two different sets of dielectric parameters for comparison. Significant differences cannot be appreciated between the two diagrams. This is due to the fact that ΔS is slightly dependent on the dielectric contrast between malignant and normal tissue, which is lower for the second group of dielectric properties, while it mainly depends on the over-temperature localized in the tumor volume [11].

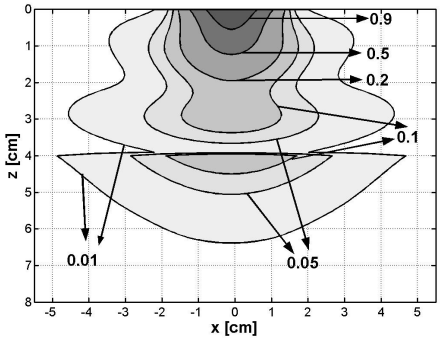

(a)

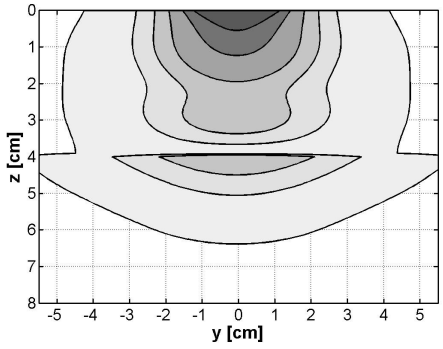

(b)

Fig. 7. Contour-level diagrams of $P_d=1/2\ \sigma\ |E|^2$ on the principal plane perpendicular a) and parallel b) to the aperture field, respectively. For normal breast: ε_{rb}=10, σ_b=0.2 *S/m*, for muscle : ε_{rm}=50, σ_m=1.5 *S/m* [32].

The diagrams in Fig. 9(a) refer to the compressed breast and to the adiabatic (bold line) and steady-state (gray line) temperatures. A realistic curve for ΔS lies between these diagrams. A tumor is radiometrically visible if the difference signal overcomes the resolution, i.e. $\Delta S > \delta S$ is the condition for a tumor to be visible. A reference value can be δS =0.1°C with 1s integration time. We conclude that the visibility of a 10mm tumor increases passing from about 25mm (Fig. 8) in the undeformed breast to a value between 30mm and 38mm in the deformed breast and 35% net deformation if the dielectric parameters are chosen as in [11] (between 30 and 45mm with parameters in [34, 35], Fig. 9(b)). ΔS is greater when the second group of parameters is considered due to the shift of the maximum of P_d, as shown in Fig. 10.

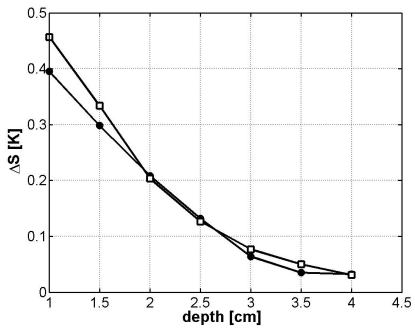

Fig. 8. Difference radiometric signal (unhealthy-normal) of a 10mm lesion vs. depth and a 3cm aperture antenna for non-compressed breast. The line with circles refers to ε_{rb}=10, σ_b=0.2 *S/m* for normal breast and ε_{rb}=50, σ_b=1.5 *S/m* for malignant breast, as in [11], while the line with diamonds refers to ε_{rb}=39, σ_b=1.18 *S/m* for normal breast [34] and ε_{rb}=55, σ_b=2 *S/m* for malignant breast [35].

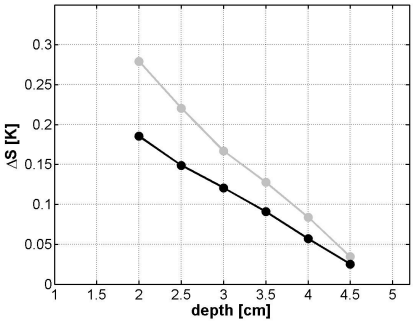

(a)

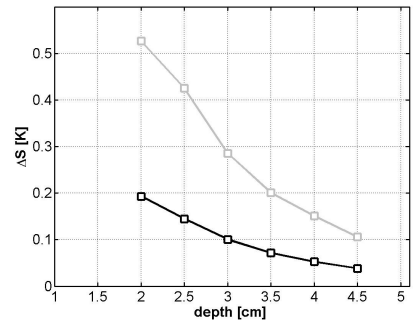

(b)

Fig. 9. Difference radiometric signal ΔS (unhealthy-normal) of a 10mm lesion vs. depth and a 3cm aperture antenna for compressed breast: adiabatic temperature (bold line), steady-state temperature (gray line). Dielectric parameters a) as in [11], b) as in [34,35]. 35% net deformation.

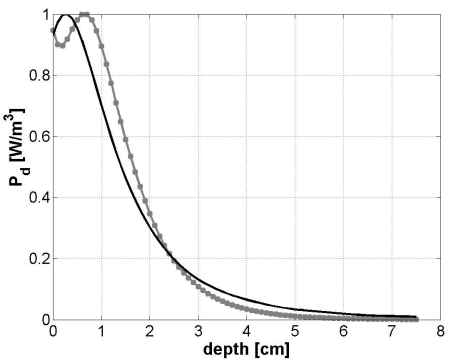

Fig. 10. Normalized P_d along the z-axis passing through the center of a 3cm aperture for undeformed breast. Dielectric parameters (bold line) as in [11], (gray line) as in [34].

V. CONCLUSION

The problem of estimating the visibility of a breast tumor by a passive radiometric device has been addressed when the sensing antenna is pressed against the breast. A mechanical and thermal model of the breast under compression by the contacting antenna has been developed, based on the data available in the literature. The mechanical behavior has been modeled by a non-linear constitutive equation, while the temperature satisfies the classical bio-heat equation. Both problems have been solved in a finite-element frame. The thermal radiation that is received by an ideal radiation-balance radiometer has been estimated solving the electromagnetic problem of antenna radiation onto the breast. According to the results of the numerical analysis, the excess in radiometric signal due to a 10mm tumor overcomes a typical radiometric resolution to a depth between 3 and 4 cm in the case of 35% compression. The above analysis has assumed that the tissue mechanical, thermal and electric properties are uniform within the normal breast.

REFERENCES

[1] F. Bardati and D. Solimini, "Radiometric sensing of biological layered media," *Radio Sci.*, vol. 18, no. 6, pp. 1393-1401, 1983.

[2] F. Sterzer, P. Paglione, F. Wozniak, J. Mendecki, E. Friedenthal, and C. Botstein, "Self-balancing microwave radiometer for non-invasively measuring the temperature of subcutaneous tissue during localized hyperthermia treatments of cancer," *IEEE MTT-S Int Microwave Symp Digest*, vol. 82, no. 1, pp. 438-440, 1982.

[3] M. Chivè, M. Plancot, Y. Leroy, G. Giaux, and B. Prevost, "Microwave (1 and 2.45 GHz) and radiofrequency (13.56 MHz) hyperthermia monitored by microwave thermography," *12th European Microwave Conf*, Helsinki (Finland), Sept. 1982.

[4] S. Jacobsen, P. Stauffer, and D. Neuman, "Dual-mode antenna design for microwave heating and non-invasive thermometry of superficial tissue disease," *IEEE Trans Biomed. Eng.*, vol. 47, no. 11, pp. 1500-1509, 2000.

[5] C. Gros, M. Gautherie, and P. Bourjat, "Prognosis and post-therapeutic follow-up of breast cancers by thermography," *IEEE Trans Biomed Eng*, vol. 6, pp.77-90, 1975.

[6] J. Edrich, "A millimeter-wave thermography for human breast and spine scans," *6th European Microwave Conf*, Rome, pp. 137-140, Sept. 1976.

[7] A. H. Barret, P. C. Myers, and M. L. Sadowsky, "Detection of breast cancer by microwave radiometry," *Radio Sci.*, vol. 12, no. 6(S), pp. 167, 1977.

[8] K. L. Carr, A. M. El-Mahdi, and J. Shaffer, "Dual-mode microwave system to enhance early detection of cancer," *IEEE Trans Microwave Theory Tech*, vol. 29, no.3, pp. 256-260, 1981.

[9] J. W. Lee, S. M. Lee, K. S. Kim, W. T. Han, G. Yoon, L. A. Pasmanik, I. A. Ulyanichev, and A. V. Troitsky, "Experimental investigation of the mammary gland tumor phantom for multifrequency microwave radio-thermometers," *Med Biol Eng Comput*, vol. 42, no.5, pp. 581-590, 2004.

[10] K. M. Ludeke, J. Kohler, and J. Kanzenbach, "A new radiation balance microwave thermograph for simultaneous and indipendent temperature and emissivity measurements," *J Microwave Power*, vol. 14, pp. 117-121, 1979.

[11] F. Bardati and S. Iudicello, "Modeling the visibility of breast malignancy by a microwave radiometer," to be published on *IEEE Trans. Biomed. Eng.*

[12] F. Bardati and S. Iudicello, "Modeling functional imaging of breast by microwave radiometry," *ACES Conference*, Verona, Italy, pp. 871-875, 19-23 Mar. 2007.

[13] "The European Protocol for the Quality Control of the Physical and Thecnical Aspects of Mammography Screening." CEC Report EUR 14821, 3rd edn 1999. http://ikrweb.uni-uenster.de/aqs/Richtlinien /qualitaet_mammo/qualitaet_mammo.html

[14] G . M. J. Van Leeuwen, J. W. Hand, J. B. Van de Kamer, and S. Mizushina, "Temperature retrieval algorithm fro brain temperature monitoring using microwave brightness temperatures," *Electronics Letters*, vol. 37, no. 6, pp. 341-2, 2001.

[15] COMSOL, www.comsol.com, Version 3.3a.

[16] A. Samani, J. Bishop, M. J. Yaffe, and B. Plewes, "Biomechanical 3-D finite element modeling of the human breast using MRI data," *IEEE Transactions on Medical Imaging*, vol. 20, no. 4, pp. 271-279, 2001.

[17] N. V. Rviter, T. O. Muller, R. Stotzka, H. Gemmeke, J. R. Reichenba, and W. A. Kaiser, "Automatic image matching for breast cancer diagnostics by a 3D deformation model of the Mamma," *Biomed. Tech.* (Berl), 47 Suppl1 Pt2, pp. 644-7, 2002.

[18] P. Pathmanathan, D. Gavaghan, J. Whiteley, S. M. Bredy, M. Nash, P. Nielsen, and V. Rajagopal, "Predicting tumor location by simulating large deformations of the breast using a 3D finite element model and nonlinear elasticity," *Proc. MICCAI2004, LNCS3217, Springer-Verlag,* pp. 217-224*,* 2004.

[19] V. Rajagopal, P. M. F. Nielsen, and M. P. Nash, "Development of a three dimensional finite element model of breast mechanics," *Proceedings of the 26th Annual*

International Conference of the IEEE EMBS, San Francisco, CA, USA, 1-5 Sept. 2004.

[20] N. V. Ruiter, R. Stotzka, T. O. Muller, H. Gemmeke, J. R. Reichenbach, and W. A. Kaiser, "Model-Based registration of X-Ray Mammograms and MR images of the female breast," *IEEE Transactions on Nuclear Science*, vol. 53, no. 1, pp. 204-211, Feb. 2006.

[21] V. Vuskovic and M. Kauer, "In vivo-measurement of elasto mechanical properties of soft biological tissue," in *European Medical and Biological Engineering Conference*, Vienna, Austria, 1999.

[22] R. D. Howe, "Identification of constitutive nonlinear constitutive law parameters of breast tissue," in *Summer Bioengineering Conference*, Vail, Colorado, 22-26 June 2005.

[23] N. Ruiter, "Registration of X-Ray Mammograms and MR-volumes of the female breast based on simulated Mammographic deformation." *PhD thesis*, pp. 55-74, University of Mannehim, 2003.

[24] D. C. Sullivan, C. A. Beam, S. M. Goodman, and D. L. Watt, "Measurement of force applied during Mammography," *Radiology*, vol. 181, no. 2, pp. 355-357, 1991.

[25] P. Wellman, R. D. Howe, E. Dalton, and K. A. Kern, "Breast tissue stiffness in compression is correlated to histological diagnosis," *Tech. Rep.*, Harward BioRobotics Laboratory, Harward University, Cambridge, Mass, USA, 1999.

[26] A. R. Mijar, J. S. Arora, "An Augmented Lagrangian optimization method for conact analysis problem, 1: formulation and algorithm," Struct Multidisc Optim, vol. 28, pp. 99-112, 2004.

[27] E. Y. K. Ng and N. M. Sudharsan, "An improved three dimensional direct numerical modeling and thermal analysis of a female breast with tumor," *Proc. Instn Mech Engrs*, vol. 215, no. 1, pp. 25-37, 2001.

[28] T. Yahara, T. Koga, S. Yoshida, S. Nakagawa, H. Deguchi, and K. Shirouzu, "Relationship between microvessel density and thermographic hot areas in breast cancer," *Surg Today*, vol. 33, pp. 243–248, 2003.

[29] M. Gautherie, Y. Quenneville, and C. M. Gros, "Metabolic heat production growth rate and prognosis of early breast carcinomas," *Biomedicine*, vol. 22, pp. 328–336, 1975.

[30] W. B. Nickell, J. Skelton, "Breast fat and fallacies: more than 100 years of anatomical fantasy," *J of Hum Lact*, vol. 21, no. 2, pp. 126-130, 2005.

[31] N. A. Lee, H. Rusinek, J. Weinreb, R. Chandra, H. Toth, C. Singer, and G. Newstead, "Fatty and Fibroglandular tissue volumes in the breast of women 20-83 years old: comparison of X-Ray Mammography and computer-assisted MR imaging," *AJR*, vol. 168, no. 2, pp. 501-6, 1997.

[32] S. Gabriel, R. W. Lau, and C. Gabriel, "The dielectric properties of biological tissues: II. Measurements in the frequency range 10 Hz to 20 GHz ," *Phys. Med. Biol.*, vol.41, no. 41, pp. 2251-2269, 1996.

[33] X. Li and S. C. Hagness, "A confocal microwave imaging algorithm for breast cancer detection," *IEEE Microwave Wireless Compon. Lett.*, vol. 11, no. 3, pp. 130–132, Mar. 2001.

[34] M. Lazebnik, L. McCarteney, D. Popovic, C. B. Watkins, M. J. Lindstrom, J. Harter, S. Sewall, A. Magliocco, J. H. Booske, M. Okoniewsky, and S. C. Hagness, "A large-scale study of the ultrawideband microwave dielectric properties of normal breast tissue obtained from reduction surgeries," *Phys. Med. Biol.*, vol. 52, pp. 2637-2656, 2007.

[35] M. Lazebnik, L. McCarteney, D. Popovic, L. McCarteney, C. B. Watkins, M. J. Lindstrom, J. Harter, S. Sewall, T. Ogilvie, A. Magliocco, T. M. Breslin, W. Temple, D. Mew, J. H. Booske, M. Okoniewsky, and S. C. Hagness, "A large-scale study of the ultrawideband microwave dielectric properties of normal, benign and malignant breast tissues obtained from cancer surgeries," *Phys. Med. Biol.*, vol. 52, pp. 6093-6115, 2007.

[36] B. Bocquet, A. Mamouni, M. Hochedez, J. C. Van de Velde, and Y. Leroy, "Visibility of local thermal structures and temperature retrieval by microwave radiometry," *Elettronics Letters*, vol. 22, no. 3, pp. 120–121, 1986.

[37] P. C. Myers, N. L. Sadowsky, and A. H. Barrett "Microwave Thermography: Principles, Methods, and Clinical Applications," *J. Microwave Power*, vol. 14, no. 2, pp. 105-115, 1979.

[38] D. V. Land, S. M. Fraser, and R. D. Shaw "A review of clinical experience of microwave Thermography," *J. Med. Eng. Tech.*, pp. 109-113, 1986.

[39] S. Mizushina, Y. Hamamura, and T. Sugiura "A three-band microwave radiometer system for noninvasive measurement of the temperature at various depths," *IEEE MTT-S Digest.*, vol. 86, no. 1, pp. 759-762, 1986.

Santina Iudicello received the M.S. degree in medical engineering from the Universita di Roma Tor Vergata, Italy, in 2005. She currently is a PhD student with interests in the microwave and radiofrequency techniques for diagnosis and therapy of breast cancer.

Fernando Bardati was born in Rome, Italy, in 1941. He received the Laurea in Electronic Engineering (in 1965) and the Libera Docenza in Microwaves from the University of Rome in 1971. He was Assistant/Associate Professor of Electronics and of Electrical Measurement at the Universities of L'Aquila and Rome from 1973 to 1985. He currently is Full Professor of Electromagnetic Fields at the University of Rome Tor Vergata. In 1995 he was a visiting professor at the Oncological Department of the University of Arizona in Tucson. From 1980 he worked in medical applications of microwaves, such as antitumoral hyperthermia and the inverse problem of microwave radiometry. He has been involved with research in electromagnetic field propagation modeling in complex environments. His current research is focused on the development of a new generation clinical radiometer for temperature monitoring during thermal treatments and for early cancer diagnosis.